

Irregular transcription dynamics for rapid production of high-fidelity transcripts

Martin Depken

*Department of Bionanoscience, Kavli Institute of Nanoscience,
Delft University of Technology, Delft, The Netherlands*

*Department of Physics and Astronomy, Vrije Universiteit,
De Boelelaan 1081 1081 HV, Amsterdam, The Netherlands and*

Max Planck Institute for the Physics of Complex Systems, Nöthnitzerstrasse 38, 01187 Dresden, Germany

Juan M. R. Parrondo

*Departamento de Física Atómica, Molecular y Nuclear and GISC,
Universidad Complutense de Madrid, 28040-Madrid, Spain and*

Max Planck Institute for the Physics of Complex Systems, Nöthnitzerstrasse 38, 01187 Dresden, Germany

Stephan W. Grill

*Max Planck Institute for the Physics of Complex Systems,
Nöthnitzerstrasse 38, 01187 Dresden, Germany and*

Max Planck Institute of Molecular Cell Biology and Genetics, Pfotenhauerstr. 108, 01307 Dresden, Germany

Both genomic stability and sustenance of day-to-day life rely on efficient and accurate readout of the genetic code. Single-molecule experiments show that transcription and replication are highly stochastic and irregular processes, with the polymerases frequently pausing and even reversing direction. While such behavior is recognized as stemming from a sophisticated proofreading mechanism during replication, the origin and functional significance of irregular transcription dynamics remain controversial. Here, we theoretically examine the implications of RNA polymerase backtracking and transcript cleavage on transcription rates and fidelity. We illustrate how an extended state space for backtracking provides entropic fidelity enhancements that, together with additional fidelity checkpoints, can account for physiological error rates. To explore the competing demands of transcription fidelity, nucleotide triphosphate (NTP) consumption and transcription speed in a physiologically relevant setting, we establish an analytically framework for evaluating transcriptional performance at the level of extended sequences. Using this framework, we reveal a mechanism by which moderately irregular transcription results in astronomical gains in the rate at which extended high-fidelity transcripts can be produced under physiological conditions.

As organisms evolved and diversified, more genes, longer genes and bigger genomes needed to be processed [1], with increased demands on fidelity. Central to fidelity in replication and transcription is that the four different NTPs possess different affinities for pairing with template nucleotides. This results in a preference for forming proper Watson-Crick pairs [2]. Although substantial [3], this selectivity is ultimately limited by early and immutable evolutionary choices pertaining to the chemistry of nucleotides. To meet further demands for fidelity, both DNA and RNA polymerases have evolved proofreading mechanisms capable of removing errors which have already been incorporated into their growing polymer product. Through such mechanisms, replication reaches an error ratio (number of incorrect bases divided by the number of correct bases in the final transcript) of the order of $1/10^8$ [4], while transcription achieves error ratios of the order of $1/10^5$ [5]. In this paper we seek to provide a quantitative understanding of transcriptional proofreading and its consequences for nucleotide consumption and transcription speed. Due to the incomplete data concerning the microscopic rates for any individual type of polymerase, we here rely on the great structural homology among bacterial, eukaryotic, and archaeal polymerases to [6, 7] to infer *order-of-magnitude* estimates of transition rates between micro-

scopic states for a generic polymerase.

The theoretical underpinning of kinetic proofreading was established by Hopfield over 30 years ago [8]. However, the standard treatment assumes the bases to be repeatedly checked *before* being *permanently* incorporated into the growing transcript. This pre-incorporation selection (PIS) results in an ever growing transcript. With the event of single-molecule techniques, it is now well established that both RNA and DNA polymerases elongate their produce in a highly irregular manner: repeatedly pausing, moving backwards, and cleaving bases from the growing molecule [9–18]. In fact, post-incorporation proofreading (PIP) has long been recognized to play a vital role in error suppression [5, 9, 11, 17, 19, 20], but has received little attention at a quantitative theoretical level [21].

We here use stochastic modeling to explore the downstream effects of PIP in transcription, and the connection between proofreading, irregular transcription dynamics, and overall elongation performance. Our stochastic hopping model [21, 22] is built using structurally well characterized states, with transition rates measured in physiologically relevant settings. The model quantitatively couples chain elongation to the observed depolymerizing action of proofreading [9, 11]. Through this we show that the highest error-suppression calculated within a stan-

standard Hopfield scheme corresponds to a pathological situation with a net shortening of the transcript over time—a fact previously overlooked. This highlights the importance of moving beyond considerations of fidelity alone if we are to gain even a qualitative understanding of this fundamental process.

Proofreading must be efficient on a wide variety of genes, and we adopt a sequence-averaged view to identify a mechanism that works on generic sequences. Through this we are able to separate the dynamically generated heterogeneity from that of a static, sequence based, origin. We show that the dynamics of an *efficiently* transcribing polymerase should be expected to be irregular—even before taking sequence effects into account. This suggests that a substantial part of the heterogeneous dynamics seen in single-molecule experiments is functionally advantageous and important for ensuring fidelity [5, 9, 11–14, 23].

I. MODELING ERROR SUPPRESSION THROUGH PIS AND PIP

Thermal fluctuations are significant on the molecular scale, and we describe transcription as a stochastic hopping process between well defined states, with transition rates set by the intervening free-energy barriers [24]. Following Hopfield [8], we take the error suppression to be achieved through a sequence of serially connected energy-consuming, molecular-scale, and error-correcting checkpoints. The quality of a checkpoint is judged by its error fraction r , and the quality of several sequential checkpoints is given by the product of individual error fractions $r_1 \cdot r_2 \cdot r_3 \cdot \dots$ (see supplemental information).

Error suppression in transcription involves several checkpoints, divided into two classes: PIS and PIP [5]. Contrary to the situation for the DNA polymerase, both types of checkpoints are controlled by the same multifunctional active region inside the RNA polymerase (RNAP) [25, 26]. The PIS process likely involves several steps [5] before the incoming NTP establishes the correct Watson-Crick base pairing with the DNA template, and catalyzes onto the growing RNA molecule [5, 27]. As the states prior to catalysis are limited by the free-energy cost ΔG_{act} of binding the wrong base to the template DNA strand within the polymerase, $r_{\text{PIS}} \geq \exp(-\Delta G_{\text{act}}/k_{\text{B}}T)$. From direct nucleotide discrimination studies r_{PIS} has been shown to be $1/10^3 - 1/10^2$ [3], corresponding to an average $\Delta G_{\text{act}} \approx 6k_{\text{B}}T$. Utilizing PIS alone, sequences of no more than a few hundred base pairs (bp) can be reliably transcribed without errors.

To increase fidelity past r_{PIS} , and be able to faithfully transcribe longer genes, RNAP has evolved the ability to proofread the transcript by selectively removing already incorporated bases [5, 9, 11]. The successive action of both PIS and PIP is known to bring the combined error fraction $r_{\text{PIS}}r_{\text{PIP}}$ down to around $1/10^5$ [28–30]. From the estimates of the PIS efficiency mentioned above,

we expect half of the error suppression to reside in PIP: $r_{\text{PIP}} = 1/10^3 - 1/10^2$. Lead by experimental results we now set out to quantitatively explain how this is achieved in a physiologically relevant setting through the use of extended, backtracked pauses. To highlight the benefits and implications of an extended backtracked state space, we first consider the case of only one backtracked state, and later contrast it to the case with the physiologically more relevant case of multiple states.

A. Proofreading through backtracking

It is well established that an erroneous base can be cleaved from the growing transcript once the polymerase has entered what is known as a backtracked state[50] (see Figure 1A): an off pathway state where the whole polymerase is displaced backward along the transcript [15, 23]. Within the polymerase, the template DNA and nascent RNA strands form a 8-9 bp hybrid. As the polymerase shifts backward, this hybrid remains in register by breaking the last formed bond and reforming an old bond at the opposite end of the hybrid [14, 15, 23] (see Figure 1B and C). This exposes already incorporated bases to the active site, blocking further elongation but enabling cleavage of the most recently added base (catalyzed by the transcription factor IIS in eukaryotes and GreA and GreB in prokaryotes) [11, 20, 25, 26, 32–35]. If cleaved, a potential error is removed, the active site is cleared, and elongation can resume. The cleavage process competes with the spontaneous recovery from the backtrack [15], by which the polymerase returns to the elongation competent state without removing the potential error (see Figure 1C). In order for cleavage from the backtracked state to lower the error content, the cleavage reaction must select for erroneous bases. The inability of incorrectly matched bases to form proper Watson-Crick base pairing within the RNA-DNA hybrid induces this selectivity. If an error has been catalyzed onto the 3'-end of the nascent RNA molecule, the total energy of the transcription complex is lowered if the RNAP moves into a backtrack (see Figure 1D). Doing this, the RNAP extrudes the unmatched base pair from the hybrid and so returns to the low energy state of a perfect Watson-Crick base-pairing within the entire hybrid (see Figure 1C). When the polymerase is in a backtracked state, the last added base is exposed to the active site and can be cleaved off.

How much cleavage from backtracked states contributes to error suppression depends on the effect of misincorporations on the transition rates in and out of backtracks. Specifically, the manner in which a misincorporation affects the transition state to backtracking determines if fidelity increases will be affected through an increased entrance rate into the backtrack (no shift of transition state) or a lowered exit rate out of the backtrack (transition state shifts with the hybrid energy). For the latter case to have an appreciable proofreading capability,

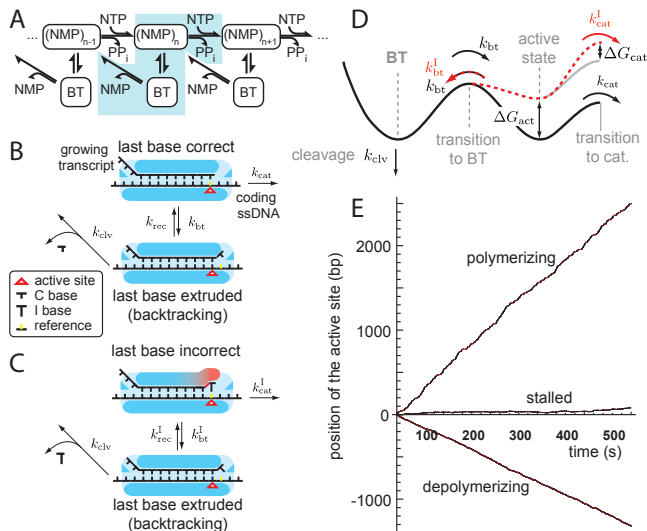


FIG. 1: Single-state backtracking. A) The basic hopping model coupling one-step backtracking to elongation. The repetitive unit is highlighted, with the off-pathway backtracked state indicated as BT. After entering a backtrack, elongation can resume either through cleavage out to a previous state of the chain $(\text{NMP})_{n-1}$ or by recovery without cleavage to the entrance state $(\text{NMP})_n$. B) Schematic illustration of the repeat unit with a correct base incorporated last. The template strand, the nascent transcript, and the hybrid region of the polymerase are shown. The polymerase can enter a backtrack with rate k_{bt} or add a base to the transcript with rate k_{cat} . From the backtracked state, recovery by cleavage occurs with rate k_{clv} , while realigning without cleavage occurs at a rate k_{rec} . C) Same as B, but with an incorrect base at the growing 3'-end of the transcript. The corresponding rates are indicated with the superscript I. D) Sketch of the free-energy landscape corresponding to B and C. Solid black line corresponds to the last base correct; dashed red line corresponds to the last base incorrect. ΔG_{act} refers to the free-energy increase at the active site when the last incorporated base is wrong, while ΔG_{cat} denotes the corresponding increase in the barrier to catalysis (cat). Recovery without cleavage occurs at a rate k_{bt} , which places all selectivity in the entrance step to the backtrack (see text). E) Three traces simulated with a Gillespie algorithm: a typical polymerizing RNAP with ($k_{cat} = 10/\text{s}$, $k_{bt} = 1/\text{s}$, $k_{clv} = 0.1/\text{s}$, see main text), a stalled polymerase ($k_{cat} = 1/\text{s}$, $k_{bt} = 10/9\text{s}$, $k_{clv} = 10/\text{s}$), and a depolymerase ($k_{cat} = 1/\text{s}$, $k_{bt} = 10/\text{s}$, $k_{clv} = 10/\text{s}$). Traces are black when the polymerase is elongating, and red when backtracked.

every single base must at some point be extruded out of the polymerase through backtracking, such that the base can be proofread and removed if it happen to be incorrectly matched to the template strand. The required high backtracking frequency would render the polymerization process inefficient—even reverse it (see below)—which is clearly not what is observed in experiments [15, 36]. We thus take the selectivity to reside in the entrance step of the backtrack (see Figure 1D). For rates as illustrated in

Figure 1B and C, this corresponds to $k_{rec} = k_{rec}^I = k_{bt}$ and $k_{bt}^I = k_{bt} \exp(\Delta G_{act}/k_B T)$ (rates corresponding to incorrect bases are denoted with the superscript I). We will simply refer to k_{bt} as the backtracking rate, and the resulting form of the free-energy landscape is illustrated in Figure 1D.

B. Physiological rate estimates

Although single-molecule traces give us direct access to many of the individual rates introduced in Figure 1B and C, the spread even between individual enzymes of any specific type of polymerase is substantial [37, 38]. On top of this, not all rates are known for any one type of polymerase, so we are here content with relying on the structural homology between polymerases [6, 7] and take *in vitro* rates from the different domains as representing order of magnitude estimates of a generic enzyme. We use $k_{cat} = 10/\text{s}$ [37, 38] (prokaryotic) [15] (eukaryotic), backtracking rate $k_{bt} = 1/\text{s}$ [39] (prokaryotic), and cleavage rate $k_{clv} = 0.1/\text{s}$ [15] (eukaryotic). Though this will not cover every scenario, the analytical nature of our work enables direct application of our results to other relevant situations.

In a development largely parallel to the theory of kinetic proofreading through PIS [8], the error suppression of PIP can be calculated as (see supplemental information)

$$r \simeq \frac{k_{cat}}{k_{cat} + k_{clv} e^{(\Delta G_{act} + \Delta G_{cat})/k_B T}}. \quad (1)$$

Here ΔG_{cat} denotes the change in barrier height for the transition to catalysis when trying to incorporate a base directly after an error (see Figure 1D). We can get an estimate of ΔG_{cat} from published experiments that use "non-hydrolyzable" nucleotide substitutes. These substitutes are thought not to influence binding affinities, but to change the catalysis rate to an extent comparable to that of an erroneous base [11]. From this we estimate $\Delta G_{cat} \approx 2k_B T$. For our typical polymerase this implies proofreading capabilities amounting to a modest $r_{PIP} \approx 1/30$: off by an order of magnitude from the experimentally determined fidelity ($1/10^3 - 1/10^2$). Note that the error ratio is insensitive to k_{bt} for our typical polymerase ($k_{cat} \gg k_{bt} \gg k_{clv}$). Further, a comparison of the regular traces (see Figure 1E) resulting from this model (see Figure 1A) with those from single-molecule experiments [15, 17, 39] demonstrates that the model does not adequately capture the observed irregular transcription dynamics (see also below). Although much of the observed dynamical heterogeneity has been attributed to structural heterogeneity through sequence specific pauses [17, 37, 40], we here show that this is not *necessarily* the dominant contribution.

C. Entropic fidelity enhancements

It is clear from Equation 1 that apart from increasing the energy penalty for a bad basepair, a low error-ratio can be achieved through a relative increase of the transcript cleavage rate compared to the elongation rate. Given their reverse arrangement ($k_{\text{cat}} \simeq 10/\text{s} \gg k_{\text{clv}} \simeq 0.1/\text{s}$), we speculate that the evolution of these rates has been strongly limited by external constraints pertaining to nucleotide chemistry and the intercellular environment. To mediate these external constraints, the polymerase has had to find alternative *internal* paths to increase error suppression.

One such internal path could be to reduce the free energy of the backtracked state. This would suppress spontaneous reversal of the backtrack and therethrough increase the probability of cleavage and error removal. Since a substantial part of the free energy relates to the energetics of base matching within the hybrid, the energy level of the backtracked state is likely constrained by the structure of the hybrid—again presumably fixed by early evolutionary choices. However, nature appears to have come up with a different solution: an effective entropic reduction in the free-energy level of the backtracked state is achieved by extending the number of accessible states. RNAP is able to backtrack by more than just one base, and thermally move between the different backtracking states that are available [15, 23, 41–43] (see Figure 2A). With N off-pathway and backtracked proofreading states, the free energy associated with the backtracked state would, in an equilibrium setting, be reduced by the entropic term $k_B T \ln(N)$. Even in our out of equilibrium setting this mechanism delays spontaneous recovery and raises the chance of cleavage and error removal (see supplemental information). With an extended backtracking space [51], it is now clear from simulated traces (Figure 2C) that the irregular dynamics of our typical polymerase qualitatively matches the irregular dynamics observed in single-molecule experiments [17, 37, 40] (see below for a quantitative assessment). By comparing the experimental effects of cleavage stimulating factors and simulated traces for increased cleavage rates, we provide further support of our kinetic scheme in the supplemental information. We also show that our model can capture the stalling dynamics of a polymerase as it transcribes against an increasing force [15].

When acting through extended backtracked states, the error suppression of PIP can be calculated as (see supplemental information)

$$r_{1:\text{PIP}} \simeq \frac{k_{\text{cat}}}{k_{\text{cat}} + \sqrt{k_{\text{clv}} k_{\text{bt}}} e^{(\Delta G_{\text{act}} + \Delta G_{\text{cat}})/k_B T}} \quad (2)$$

$$= \frac{k_{\text{cat}}}{k_{\text{cat}} + k_{\text{bt}} e^{\Delta G_{1:\text{PIP}}/k_B T}},$$

$$\Delta G_{1:\text{PIP}} = \Delta G_{\text{act}} + \Delta G_{\text{cat}} - \frac{1}{2} k_B T \ln(k_{\text{bt}}/k_{\text{clv}}). \quad (3)$$

Comparing Equation 2 to Equation 1, we see that fidelity is increased by extending the space available for

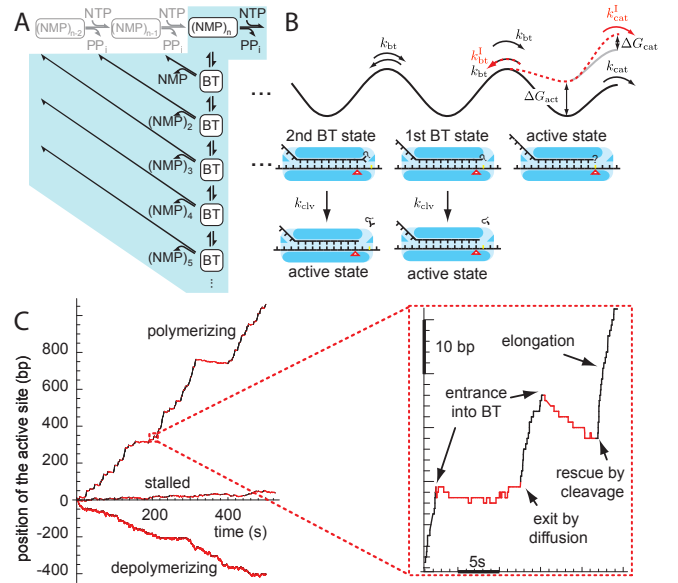


FIG. 2: Multi-state backtracking. A) The basic repeat unit of multi-state backtracking in a nested scheme. For visual clarity, only the backtracked states in the highlighted repeat unit are drawn. B) Sketch of the free-energy landscape of a multi-state backtrack. Solid black line corresponds to the last base correct; dashed red line corresponds to the last base incorrect. Also illustrated are the multiple backtracked states and the effect of cleavage. See caption to Figure 1B for a description of the rates. C) Three traces simulated with a Gillespie algorithm: a typical polymerizing RNAP with ($k_{\text{cat}} = 10$, $k_{\text{bt}} = 1$, $k_{\text{clv}} = 0.1$), a stalled complex ($k_{\text{cat}} = 10$, $k_{\text{bt}} = 10$, $k_{\text{clv}} = 0.1$), and a depolymerizing one ($k_{\text{cat}} = 1$, $k_{\text{bt}} = 10$, $k_{\text{clv}} = 0.1$)—all in accordance to the theoretical predictions derived in the supplemental information. A section of the trace for our typical polymerase has been magnified, showing two backtracks, one rescued to elongation by cleavage and one by diffusion. Only the backtrack reentering elongation through cleavage would have corrected an error at the end of the transcript. Traces are black when the polymerase is elongating, and red when backtracked.

backtracking: the low cleavage rate k_{clv} is replaced by the geometric mean $\sqrt{k_{\text{clv}} k_{\text{bt}}}$. This increases the fidelity by about a factor of three for our typical polymerase, and provides an error reduction of $r_{1:\text{PIP}} \simeq 1/100$. The notation in Equation 3 is introduced to facilitate the extension to several PIP checkpoints presented in the next section. The error suppression now depends on the additional parameter k_{bt} (c.f. Equation 1)—a parameter independent of nucleotide chemistry and susceptible to change through evolutionary pressures. Although the extension of the backtracking space does provide for fidelity enhancements, the total fidelity is still at the lower end of what is experimentally observed. However, our extended backtracking space gives further proofreading benefits by supplying the polymerase with additional inherent PIP checkpoints, as we now discuss.

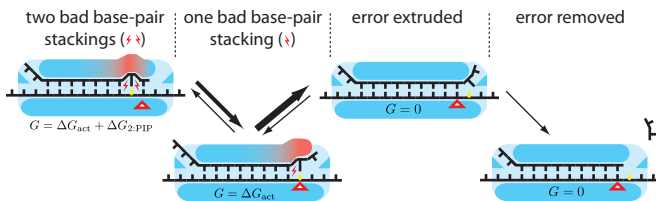


FIG. 3: **A second PIP checkpoint.** The polymerase is expected to be sensitive to errors incorporated also next to last. The magnitude of the rates are illustrated by relative thickness of the transition arrows, bad base stackings are indicated in red. G indicates the free energy of the complex with respect to the elongation competent state.

D. Second PIP checkpoint and beyond

Even when additional bases have been added to the transcript after an erroneous incorporation, the error can in principle still be corrected through an extensive backtrack and cleavage [21]. For this to lead to an appreciably increased likelihood of error removal, the random walk must be biased towards entering further into the backtrack. With an error at the *penultimate* 3'-position of the transcript, the polymerase experiences such bias, since moving into a backtrack will eliminate a bad base-pair stacking within the hybrid (see Figure 3). This is followed by another heavily biased step to completely extrude the error from the hybrid, making it amenable to cleavage. We know of no direct measurement of the penultimate bias $\Delta G_{2:\text{PIP}}$, but as the typical stacking energy in a RNA-DNA hybrid is $1.5 - 4.5 k_B T$ [2] we assume $\Delta G_{2:\text{PIP}} \approx 3 k_B T$. This second PIP checkpoint provides an error ratio (see supplemental information) of

$$r_{2:\text{PIP}} \simeq \frac{k_{\text{cat}}}{k_{\text{cat}} + k_{\text{bt}} e^{\Delta G_{2:\text{PIP}}/k_B T}}. \quad (4)$$

For our typical polymerase $r_{2:\text{PIP}} \simeq 1/3$, and the total PIP induced error reduction $r_{\text{PIP}} = r_{1:\text{PIP}} r_{2:\text{PIP}} \simeq 1/300$ falls well within the experimentally observed range.

The suggested scheme thus quantitatively accounts for the typically observed error-suppression, but there could in principle be additional inherent PIP checkpoints that would enable the polymerase to reach even higher fidelities. An increasing free-energy penalty for moving the error further into the hybrid would incur a longer range bias for backtracking, and additional fidelity gains according to (see supplemental information)

$$r_{\text{PIP}} = r_{1:\text{PIP}} r_{2:\text{PIP}} \cdots r_{n:\text{PIP}} \cdots$$

$$r_{n:\text{PIP}} \simeq \frac{k_{\text{cat}}}{k_{\text{cat}} + k_{\text{bt}} e^{\Delta G_{n:\text{PIP}}/k_B T}}. \quad (5)$$

Based on structural considerations of base pairing within the RNA-DNA hybrid, we conclude that PIP-proofreading of RNAP includes at least two serial checkpoints that account for the typical fidelities observed in

transcription. The polymerase could in principle select and remove an error as long as it remains within the hybrid. Intriguingly, the 8-9-bp hybrid might thus not only serve the purpose of stabilizing the ternary complex [45], but also provide enhanced fidelity.

E. Power-law pause distributions and spatial heterogeneity

We next illustrate the consequences of the proofreading states on pause duration and frequency. To this end we simulate our typical polymerase transcribing a long sequence and compare it to a simulation of an otherwise identical polymerase, but which has PIP turned off ($k_{\text{bt}} = 0/\text{s}$). In Figure 4A we show a particular realization (of our generic polymerase) of incorporation errors (only PIS in red) together with the errors left after the section has been proofread (PIS and PIP in black). The fidelity enhancements are clearly visible, but they come at the cost of both an decreased velocity, as well as an increased spatial heterogeneity. These effects are qualitatively visible already at the level of individual traces, but are quantitatively best seen in the changes of the dwell-time distribution (see Figure 4B) or in the transition-rate (inverse dwell-time) distribution (see Figure 4C). In the dwell-time distribution, proofreading introduces a power-law regime, throughout which the probability of a long pause falls off with duration t as $t^{-3/2}$ [39], until it drops off exponentially beyond $t \sim 1/k_{\text{clv}}$. In Figure 4B we see a clear exponential behavior of the dwell-time distribution for both processes at around $t \sim 1/k_{\text{el}} = 0.1\text{s}$, while the proofreading polymerase also has the above mentioned power-law decay extending out to $t \sim 1/k_{\text{clv}} = 10\text{s}$. Similarly, considering the transition-rate distributions we see a narrow but significant low velocity peak develop around the transition rate $\sim k_{\text{clv}} = 0.1/\text{s}$, diminishing the bare elongation peak situated around the rate $\sim k_{\text{cat}} = 10/\text{s}$ (see Figure 4C). To further elucidate the effects of the power-law regime, we consider another important observable: the pause-time distribution, or the total time a polymerase spends at each position along the DNA molecule. In Figure 4D we show pause density plots along a sequence of 500 bp, with darker bands indicating longer total time spent at that position during the transcription process. Comparing transcription with and without PIP it is clear that PIP leads to greater spatial heterogeneity, exhibiting distinct regions of markedly increased occupation density even where there are no incorporation errors. Thus, our model accounts for both the observed spatial heterogeneity as well as the broad pause-time distributions [15, 37] without the need to introduce additional assumptions about the effects of sequence heterogeneity [15, 39].

Having shown that external constraints can be mediated through accessing an internal extended backtracked space—resulting in irregular transcription dynamics—we now turn our attention to the specific level of irregu-

larity observed in experiments. Irregularity is tuned by the backtracking rate, and considering that increasing k_{bt} would render all proofreading checkpoints more effective (see Equation 5) one might wonder why the backtracking rate is kept moderate (1/s) and not made much larger [36, 39].

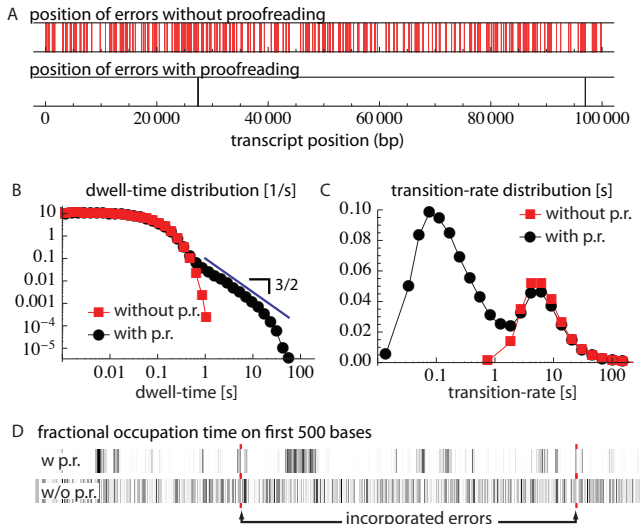


FIG. 4: **The effects of proofreading.** A) On top we show a realization of incorporation errors according to our free-energy estimates (only PIS in red), and below we show the errors that survive (or, possibly, are inserted by) the proofreading mechanisms (PIS and PIP in black). B) The dwell-time distribution from a process without proofreading and one with proofreading. Proofreading gives rise to a power-law regime significantly increasing the fraction of long-pauses. C) The transition-rate (inverse dwell-time) distribution for the same processes as in B, where the effects of proofreading can be seen through a shift from a unimodal to a bimodal distribution as many excessively slow transitions involving backtracks start influencing the kinetics. D) The pause density, or the total occupation time plotted for a 500 bp sequence transcribed by the same two polymerases as used in B and C. The darker the bands, the longer the total occupation time at that position. The scales are individually normalized to cover the range of occupation times for each polymerase. Two incorporation errors are indicated with red markers.

II. TRANSCRIPTION PERFORMANCE

We have here suggested that by utilizing *extended* backtracked states, the polymerase has overcome external constraints to suppress errors. This introduces the backtracking rate k_{bt} as a variable susceptible to evolutionary pressures. In order to understand the underlying reasons for why the backtracking rate is kept moderate, we now consider the phenotypic space made available through the extended backtracking space. The quantities needed to access polymerase performance—as it varies with the level of PIP—are calculated in the supplemental

information by using continuous time random walk theory [46]. Starting with instantaneous transcriptional efficiency measures on the level of the individual base pairs, we then consider the efficiency on extended sequences or genes. Importantly, we investigate how much faster the polymerase can produce perfect transcripts of extended sequences with PIP as compared to without PIP.

A. Performance on the level of a base pair

We are interested in the effective elongation rate, and thus calculate the average elongation rate $1/\tau_{el}$ (see supplemental information). Since there is only about one error passing through the PIS checkpoint every 500 bases, we can ignore the effect of errors on the overall elongation dynamics. We now construct the efficiency measure η_{el} ,

$$\eta_{el} = \frac{1/\tau_{el}}{k_{cat}} \simeq \frac{1 - k_{bt}/k_{cat}}{1/2 + \sqrt{1/4 + k_{bt}/k_{clv}}}, \quad (6)$$

which describes the relative slowdown due to PIP. With no PIP ($k_{bt} = 0$) the efficiency is appropriately $\eta_{el} = 1$, while it vanishes at the transition between polymerization and depolymerization $k_{cat} = k_{bt}$. At this point, elongation stops proceeding with a well defined velocity, and behaves diffusively on large lengthscales. For $k_{cat} < k_{bt}$ net depolymerization sets in. This situation is pathological, and shows that backtracking cannot dominate the dynamics even though this would be judged optimal in terms of fidelity calculated within the Hopfield kinetic proofreading scheme. The transition to non-functional polymerases can be seen in the single-molecule transcription traces presented in [52] [15], and in the simulated traces presented in Figure 2C (see also supplemental Figure S4C). Also note that the overall elongation rate increases with increasing cleavage rate, as is observed experimentally [31, 32, 47]. We next introduce an efficiency parameter for PIP,

$$\eta_{PIP} = 1 - r_{PIP},$$

which is 0 in the absence of PIP and 1 for perfect PIP. Finally, we parameterize the nucleotide efficiency of the transcription process by the ratio of final transcript length and the average number of nucleotides consumed in its production. This ratio is given by the simple expression (see supplemental information)

$$\eta_{NTP} = 1 - k_{bt}/k_{cat}.$$

The measure is unity without PIP, and vanishes at stall ($\eta_{el} = 0$).

Figure 5 shows the three efficiency measures η_{el} , η_{PIP} and η_{NTP} as functions of the backtracking rate k_{bt} (within the operational range $0 \leq k_{bt} \leq k_{cat} \approx 10$), for an otherwise typical polymerase. We see that while transcription velocity and nucleotide efficiency correlate

positively, they both correlate negatively with fidelity, directly illustrating the cost of enhancing fidelity. This hints at an underlying competition, which we now explore by considering transcription of extended sequences.

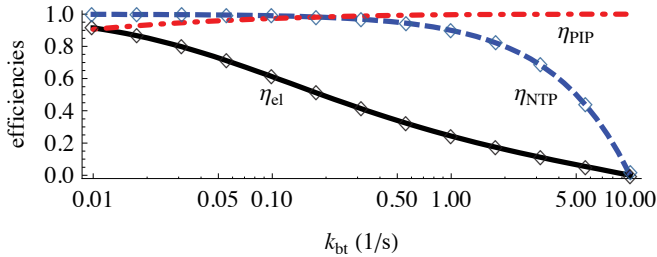


FIG. 5: **Polymerase performance.** Proofreading efficiency η_{PIP} (red dot-dashed), elongation efficiency η_{el} (black solid) and nucleotide efficiency η_{NTP} (blue dashed) as a function of the backtracking rate, for an otherwise typical polymerase with $k_{cat} = 10/s$ and $k_{clv} = 0.1/s$. Values indicated by diamonds were obtained numerically, through Gillespie simulations.

B. Performance on the level of the gene

Here we demonstrate that a moderate rate of backtracking is necessary for rapidly generating transcripts with few mistakes from extended sequences. This becomes apparent when noting that the longer the sequence, the less likely it is for a polymerase to produce an error-free transcript. It is instructive to introduce the probability P_l of producing a long error-free sequence[53] of length l . For each attempt, the probability of transcribing a sequence of length l without an error is given by $P_l(r) = (1 + r)^{-l} \simeq \exp(-lr)$, with $r = r_{PIP}r_{PIS}$ representing the total error fraction. The production-rate gain χ_{el} on extended sequences is obtained by comparing the rate at which error-free transcripts are produced with PIP, to the rate with which they are produced without PIP ($k_{bt} = 0$). Thus, $\chi_{el} = \eta_{el}P_l(r_{PIS}r_{PIP})/P_l(r_{PIS}) \simeq \eta_{el} \exp(lr_{PIS}\eta_{PIP})$. Similarly, we introduce the NTP-efficiency gain on extended genes χ_{NTP} by comparing the number of error-free transcripts produced per nucleotide used with and without PIP, giving $\chi_{NTP} = \eta_{NTP}P_l(r_{PIS}r_{PIP})/P_l(r_{PIS}) \simeq \eta_{NTP} \exp(lr_{PIS}\eta_{PIP})$. From both these quantities it is clear that even moderate PIP provides enormous gains in the rate of perfectly transcribing long ($l > 1/r_{PIS}$) sequences. With the two sequence-wide measures that we have introduced, it is now possible to address transcriptional efficiencies on the level of transcription of whole genes. As an example we consider a sequence of a length comparable to the typical human gene $l = 10^4$ bp, and in Figure 6A we plot the efficiencies χ_{el} and χ_{NTP} as a function of the backtracking rate k_{bt} (within the operational limits $0 < k_{bt} < k_{cat} = 10/s$). Each measure

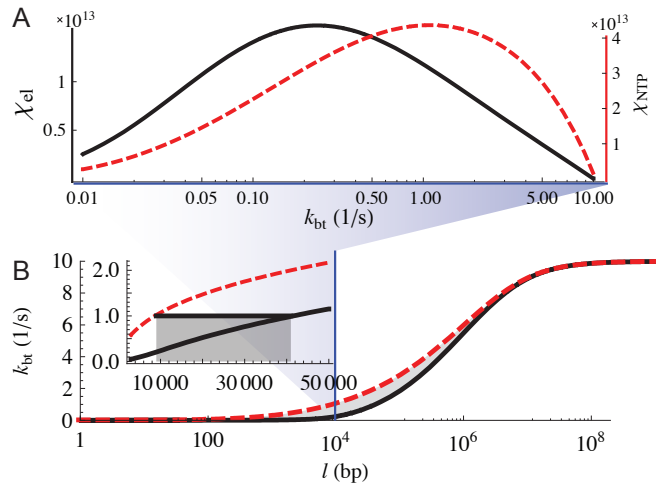


FIG. 6: **High fidelity transcript production.** A) On the left vertical axis we mark the production-rate gain on extended sequences χ_{el} as a function of the backtracking rate (black solid line). On the right vertical axis we mark the NTP-efficiency gain χ_{NTP} as a function of the backtracking rate (red dashed line), all for a sequence of length $l = 10^4$ bp. The region between the two peaks is where one might expect the optimal value of k_{bt} to lie. Note there is a gain of 13 orders of magnitude in the rate of producing error-free transcripts when transcribing with PIP as compared to without PIP, with similar gains in nucleotide efficiency. B) The backtracking rate that optimizes the production-rate gain (black solid) or the energy-efficiency gain (red dashed) as a function of sequence length. Gray shading indicates a region of compromise between both gains. Inset, a magnification of the region around $k_{bt} = 1/s$ indicates that PIP is optimal with $k_{bt} = 1/s$ for gene lengths of $10^4 - 4 \cdot 10^4$ bp. The vertical blue line indicates the sequence length used in A.

has a definite optimal value, and we see that the gains in both rate of perfect transcript production and nucleotide efficiency can be enormous, here reaching thirteen orders of magnitude. If RNAP was optimized to transcribe this particular sequence length, then we would expect the true value of the backtracking rate to lie somewhere in the intermediate region between the peaks: representing a compromise between NTP efficiency and production rate. For the intimate value of $k_{bt} = 1/s$ —coinciding with our estimate of the physiologically relevant backtracking rate—it would take a polymerase of the order of one hour to produce an error free transcript, which should be compared to 10^{13} hours without PIP.

Finally, it is interesting to ask how the region of optimal backtracking rate changes as the transcribed sequence length varies. Figure 6B shows the k_{bt} that optimizes χ_{el} (black solid line) and χ_{NTP} (red dashed line) as a function of sequence length l . The inset in Figure 6B highlights the backtracking rate for our typical polymerase ($k_{bt} = 1/s$), and the implied sequence lengths ($\simeq 10^4 - 4 \cdot 10^4$ bp) for which this backtracking rate would be optimal. A complete discussion would need

to consider relaxed fidelity constraints due to e.g. codon redundancy [48], but considering that the average gene length in eukaryotes lies in the range $10^4 - 10^5$ [1], it is thought-provoking to speculate that the moderate observed backtracking rates of around 1/s are the result of an evolutionary optimization for rapidly and efficiently producing functional transcripts from genes in the tens-of-kbp range.

III. DISCUSSION

By analytically studying a model of backtracking couple to chain elongation and cleavage, we have shown that irregular transcription dynamics is likely a result of maintaining transcriptional efficiency, not at the level of individual nucleotides, but rather, at the level of extended sequences and genes. Our work suggests that proofreading relies on an entropic enhancement of fidelity, where an extended state space reduces the chance of spontaneous recovery. This ensures low error rates even with low rates of transcript cleavage. Through backtracking, an incorporated error can be proofread at least twice through biasing the entry into backtracks, but could in principle be proofread as many times as there are bases in the RNA-DNA hybrid within the elongation complex. To what extent there are additional proofreading checkpoints beyond the two discussed here is an interesting line of future research, providing a potential link between the structure of the elongation complex and overall transcriptional efficiency and fidelity. Such work might offer additional clues as to why the RNA-DNA hybrid has a length of about 8-9 bp [49].

Considering both the effects of proofreading on NTP consumption and the production rate of extended functional transcripts, our investigation suggests that the internal hopping rate in the backtracked state is not optimized for fidelity alone. Instead, it is kept moderate in order to enable rapid production of extended transcripts that are of high fidelity. That there will

be many more backtracks than there are errors to remove is a direct consequence of undetected errors being costly, since they have the potential to render the whole transcript dysfunctional. A certain level of paranoia is thus desirable on part of the polymerase. Even though such paranoia decreases the instantaneous average transcription rate, the observed level of backtracking—perhaps counterintuitively—drastically increases the rate at which high fidelity transcripts are produced. Interestingly, the backtracking rate and the amount of backtracks in cells of a particular organism would be expected to correlate positively with the sequences length that has induced the highest evolutionary pressures on transcription (see Figure 6B, gray region). In other words, genomes with genes of increasing length should be transcribed with increasingly irregular dynamics to maintain transcriptional efficiency. It would be interesting to determine if an overall trend in backtracking rate [15, 39], and consequent irregularity of dynamics, could be found for polymerases originating in organisms with varying genetic complexity.

To conclude, our model highlights the enormous gains offered by post-incorporation proofreading when transcribing long sequences, illustrating how important this basic mechanism has become for the sustenance of life.

Acknowledgments

We thank Eric Galburt, Justin Bois and Abigal Klopfer for fruitful discussions and suggestions. JMRP acknowledges financial support from grants MOSAICO (Spanish Government) and MODELICO (Comunidad de Madrid). SWG acknowledges funding by the EMBO young investigator program and the Paul Ehrlich Foundation. MD acknowledges partial support from FOM, which is financially supported by the “Nederlandse Organisatie voor Wetenschappelijk Onderzoek”. This research was supported in part by the National Science Foundation under Grant No. NSF PHY05-51164.

-
- [1] Xu L, et al. (2006) Average gene length is highly conserved in prokaryotes and eukaryotes and diverges only between the two kingdoms. *Mol Biol Evol* 23:1107–1108.
 - [2] Sugimoto N, et al. (1995) Thermodynamic parameters to predict stability of RNA/DNA hybrid duplexes. *Biochemistry* 34:11211–11216.
 - [3] Svetlov V, Vassilyev DG, Artsimovitch I (2004) Discrimination against deoxyribonucleotide substrates by bacterial RNA polymerase. *Journal of Biological Chemistry* 279:38087–38090.
 - [4] Kunkel TA (2004) DNA replication fidelity. *Journal of Biological Chemistry* 279:16895–16898.
 - [5] Sydow JF, Cramer P (2009) RNA polymerase fidelity and transcriptional proofreading. *Current Opinion in Structural Biology* 19:732–739.
 - [6] Ebright R (2000) RNA polymerase: structural similarities between bacterial RNA polymerase and eukaryotic RNA polymerase II. *Journal of Molecular Biology* 304:687–698.
 - [7] Hirata A, Kleind BJ, Murakami KS (2008) The X-ray crystal structure of RNA polymerase from Archaea. *Nature* 451:851–854.
 - [8] Hopfield JJ (1974) Kinetic proofreading: A new mechanism for reducing errors in biosynthetic processes requiring high specificity. *Proceedings of the National Academy of Sciences of the United States of America* 71:4135–4139.
 - [9] Erie D, Hajiseyedjavadi O, Young M, von Hippel P (1993) Multiple RNA polymerase conformations and GreA: control of the fidelity of transcription. *Science*

- 262:867–873.
- [10] Donlin MJ, Patel SS, Johnson KA (1991) Kinetic partitioning between the exonuclease and polymerase sites in DNA error correction. *Biochemistry* 30:538–546.
 - [11] Thomas M, Platas A, Hawley D (1998) Transcriptional fidelity and proofreading by RNA polymerase II. *Cell* 93:627–637.
 - [12] Orlova M, Newlands J, Das A, Goldfarb A, Borukhov S (1995) Intrinsic transcript cleavage activity of RNA polymerase. *Proceedings of the National Academy of Sciences of the United States of America* 92:4596–4600.
 - [13] Zenkin N, Yuzenkova Y, Severinov K (2006) Transcript-Assisted transcriptional proofreading. *Science* 313:518–520.
 - [14] Wang D, et al. (2009) Structural basis of transcription: Backtracked RNA polymerase II at 3.4 Ångstrom resolution. *Science* 324:1203–1206.
 - [15] Galburt EA, et al. (2007) Backtracking determines the force sensitivity of RNAP II in a factor-dependent manner. *Nature* 446:820823.
 - [16] Wuite GJ, Smith SB, Young M, Keller D, Bustamante C (2000) Single-molecule studies of the effect of template tension on t7 DNA polymerase activity. *Nature* 404:103–106.
 - [17] Ibarra B, et al. (2009) Proofreading dynamics of a processive DNA polymerase. *EMBO J* 28:2794–2802.
 - [18] Kireeva ML, Kashlev M (2009) Mechanism of sequence-specific pausing of bacterial RNA polymerase. *Proceedings of the National Academy of Sciences of the United States of America* 106:8900–8905.
 - [19] Kunkel TA, Bebenek K (2000) DNA replication fidelity. *Annual Review of Biochemistry* 69:497–529.
 - [20] Jeon C, Agarwal K (1996) Fidelity of RNA polymerase II transcription controlled by elongation factor TFIIS. *Proceedings of the National Academy of Sciences of the United States of America* 93:13677–13682.
 - [21] Voliotis M, Cohen N, Molina-Pars C, Liverpool TB (2009) Backtracking and proofreading in DNA transcription. *Physical Review Letters* 102:258101.
 - [22] Greive SJ, von Hippel PH (2005) Thinking quantitatively about transcriptional regulation. *Nat Rev Mol Cell Biol* 6:221–232.
 - [23] Shaevitz JW, Abbondanzieri EA, Landick R, Block SM (2003) Backtracking by single RNA polymerase molecules observed at near-base-pair resolution. *Nature* 426:684–687.
 - [24] Risken H (1996) *The Fokker-Planck equation* (Springer).
 - [25] Kettenberger H, Armache K, Cramer P (2003) Architecture of the RNA polymerase II-TFIIS complex and implications for mRNA cleavage. *Cell* 114:347–357.
 - [26] Opalka N, et al. (2003) Structure and function of the transcription elongation factor GreB bound to bacterial RNA polymerase. *Cell* 114:335–345.
 - [27] Cramer P (2007) Gene transcription: extending the message. *Nature* 448:142–143.
 - [28] Rosenberger RF, Hilton J (1983) The frequency of transcriptional and translational errors at nonsense codons in the lacZ gene of escherichia coli. *Molecular and General Genetics MGG* 191:207–212.
 - [29] Blank A, Gallant JA, Burgess RR, Loeb LA (1986) An RNA polymerase mutant with reduced accuracy of chain elongation. *Biochemistry* 25:5920–5928.
 - [30] Mercoyrol L, Corda Y, Job C, Job D (1992) Accuracy of wheat-germ RNA polymerase II. *European Journal of Biochemistry* 206:49–58.
 - [31] Herbert KM, et al. (2010) E. coli NusG inhibits backtracking and accelerates pause-free transcription by promoting forward translocation of RNA polymerase. *Journal of Molecular Biology* 399:17–30.
 - [32] Fish RN, Kane CM (2002) Promoting elongation with transcript cleavage stimulatory factors. *Biochimica et Biophysica Acta - Gene Structure and Expression* 1577:287–307.
 - [33] Borukhov S, Lee J, Laptenko O (2005) Bacterial transcription elongation factors: new insights into molecular mechanism of action. *Molecular Microbiology* 55:1315–1324.
 - [34] Awrey DE, et al. (1998) Yeast transcript elongation factor (TFIIS), structure and function. II: RNA polymerase binding, transcript cleavage, and read-through. *The Journal of Biological Chemistry* 273:22595–22605.
 - [35] Sosunov V, et al. (2003) Unified two-metal mechanism of RNA synthesis and degradation by RNA polymerase. *EMBO J* 22:2234–2244.
 - [36] Abbondanzieri EA, Greenleaf WJ, Shaevitz JW, Landick R, Block SM (2005) Direct observation of base-pair stepping by RNA polymerase. *Nature* 438:460465.
 - [37] Neuman KC, Abbondanzieri EA, Landick R, Gelles J, Block SM (2003) Ubiquitous transcriptional pausing is independent of RNA polymerase backtracking. *Cell* 115:437–447.
 - [38] Tolic-Norrelykke SF, Engh AM, Landick R, Gelles J (2004) Diversity in the rates of transcript elongation by single RNA polymerase molecules. *The Journal of Biological Chemistry* 279:3292–3299.
 - [39] Depken M, Galburt EA, Grill SW (2009) The origin of short transcriptional pauses. *Biophysical Journal* 96:2189–2193.
 - [40] Herbert KM, et al. (2006) Sequence-resolved detection of pausing by single RNA polymerase molecules. *Cell* 125:10831094.
 - [41] Nudler E, Mustaev A, Goldfarb A, Lukhtanov E (1997) The RNA-DNA hybrid maintains the register of transcription by preventing backtracking of RNA polymerase. *Cell* 89:33–41.
 - [42] Komissarova N, Kashlev M (1997) RNA polymerase switches between inactivated and activated states by translocating back and forth along the DNA and the RNA. *Journal of Biological Chemistry* 272:15329–15338.
 - [43] Komissarova N, Kashlev M (1997) Transcriptional arrest: Escherichia coli RNA polymerase translocates backward, leaving the 3' end of the RNA intact and extruded. *Proc Natl Acad Sci USA* 94:1755–60.
 - [44] Klopper AV, Bois JS, Grill SW (2010) Influence of secondary structure on recovery from pauses during early stages of RNA transcription. *Physical Review E* 81:030904.
 - [45] Nudler E (1997) The RNA-DNA hybrid maintains the register of transcription by preventing backtracking of RNA polymerase. *Cell* 89:33–41.
 - [46] Montroll EW (1987) *Fluctuation Phenomena* (North-Holland).
 - [47] Proshkin S, Rahmouni AR, Mironov A, Nudler E (2010) Cooperation between translating ribosomes and RNA polymerase in transcription elongation. *Science* 328:504–508.
 - [48] Alberts B, et al. (1998) *Essential cell biology* (Garland New York).

- [49] Kent T, Kashkina E, Anikin M, Temiakov D (2009) Maintenance of RNA-DNA hybrid length in bacterial RNA polymerases. *Journal of Biological Chemistry* 284:13497–13504.
- [50] There is some evidence in the literature for an intermediate state between elongation and backtracking [31]. However, the rates for transversing this state are similar to those for entering the backtrack, and adding such a state does not change the general dynamics of the model.
- [51] Even with infinite room for backtracking, our typical polymerase would only take around $k_{bt}/k_{clv} = 10$ diffusive backtracking steps before being cleaved off, and would reach a typical backtracking depth of around $N \approx \sqrt{k_{bt}/k_{clv}} \approx 3$. This is below the lower estimates for the distance to RNA hairpin barriers in the trailing RNA strand [44]. We are thus justified in assuming the available backtracking distance to be effectively infinite (see Figure 2A).
- [52] See Figure 3D in [15], where an opposing force was used to increase the entrance rate into the backtrack, bringing the system to stall around 14pN.
- [53] This sequence length l should not necessarily be interpreted as the complete gene length l_{gene} , but instead as the typical error-free length $l = l_{gene}/n$ that is required, where n is the number of errors acceptable during transcription of the gene.